Estonian Journal of Engineering, 2009, **15**, 4, 293–300 doi: 10.3176/eng.2009.4.06

Characterization of functional gradient structures in duplex stainless steel castings

Jyri Tiusanen[a], Kati Rissa[a], Tapio Ritvonen[b], Juha Lagerbom[b], Kaisu Keskiaho[a] and Toivo Lepistö[a]

[a] Tampere University of Technology, Department of Materials Science, Korkeakoulunkatu 6, FIN-33720 Tampere, Finland; jyri.tiusanen@tut.fi
[b] VTT, P.O. Box 1300, FIN-33101 Tampere, Finland

Received 30 June 2009, in revised form 14 October 2009

Abstract. Titanium carbide particle reinforced metal-matrix composite coatings, formed on duplex (austenitic/ferritic) stainless steel castings, were studied. These coatings, developed for wear applications, develop a functional gradient structure through a self-propagating high-temperature synthesis (SHS) of titanium carbide (TiC). This SHS-reaction was ignited in reactive inserts by the heat of liquid steel. The reactive inserts were compressed from mixtures of titanium, carbon and molybdenum powders together with iron or duplex stainless steel powders. The coating microstructure depends on the reactive insert composition. Molybdenum reduced the TiC particle diameter, and reducing the binder content reduced the areal fraction of TiC.

Key words: particle reinforced cast structure, SHS-reaction, metal-matrix composite, coating, TiC, duplex stainless steel, interface.

1. INTRODUCTION

The production of titanium carbide particle reinforced coatings on cast structures through self-propagating high-temperature synthesis reaction is an economical and efficient alternative to making wear-resistant coatings. Moore and Feng [1,2] have studied SHS extensively in their joint articles about combustion synthesis of advanced materials. Furthermore, many articles [3–7] study the wear of TiC particle reinforced metal matrix composite structures, produced by SHS. For this study, fine titanium carbide particles were produced in a steel matrix by the SHS reaction of a reactive insert. The SHS reaction was ignited by the heat of the cast steel, inside a sand mold. The SHS reaction produces a coating, which has a functional gradient structure. In the functional gradient structure, the volume fraction of TiC particles is higher at the coating surface and lower at the substrate

coating interface. Titanium carbide, which reinforces the metal matrix composite coating, is approximately ten times harder (HV ≥ 2000) than the surrounding metal matrix. As discussed by Kim [8], the rule of mixtures models iso-strain and iso-stress determines the hardness of a composite coating by the volume fraction of the hard phase material. Furthermore, as described by Gowtam et al. [6,7], Parashivamurthy et al. [3] and Zhang et al. [4], the addition of hard particles, such as titanium carbide, into a steel matrix, significantly improves the specific modulus, hardness, specific strength and wear resistance of composites.

The heat of the cast duplex stainless steel ignites the SHS reaction inside the reactive insert, which consists of titanium, carbon, molybdenum and binder powders. Once ignited, the exothermic reaction between the titanium and the carbon maintains itself as long as reactants are available ($Ti_{(s)} + C \rightarrow TiC_{(s)}$, $\Delta H^0_{298} = -184$ kJ mol^{-1}) as described in [1–3]. Binder powders, iron or duplex stainless steel, dilute the SHS reaction. The binder powders together with molybdenum act as heat sinks and enclose the formed carbides as they melt. As shown in [9,10], molybdenum enhances the adhesion of TiC particles to the matrix steel, due to its tendency to diffuse into the TiC particle surface. Furthermore, molybdenum has been reported to reduce the growth rate and the final particle size of TiC [5].

The objective of this study was to find how reactive insert composition affects the microstructure of hard coatings. This study concentrated on three aspects of the reactive insert design: the use of pure iron or duplex (austenitic ferritic) steel binder, the addition of molybdenum, and the effect of the binder amount in the insert.

2. MATERIALS AND METHODS

The nominal compositions of the used cast steel ASTM A890 4A and the duplex steel D22 binder powder are shown in Table 1. Cast batches of the samples studied had elemental compositions, which fitted the expected nominal compositions. Elemental compositions of the cast batches were analysed with Belec Lab 3000s spark emission spectrometer.

The reactive inserts consist of controlled element ratios of hard phase formers, titanium, molybdenum and carbon, and a metallic binder, iron or duplex (austenitic ferritic) stainless steel (D22); 14 wt% of molybdenum was added into ball-milled powder mixture (1 : 1 atomic ratio) of titanium and carbon. This mixture was then ball-milled together with a set amount of 8, 12 or 25 wt%, of

Table 1. Elemental compositions of the cast steel A890 4A and the binder D22, wt%

Description	Cr	Mo	Ni	C	Si	Mn	P	S	Cu
ASTM A890 4A	21.0–23.5	2.5–3.5	4.5–6.5	≤0.03	≤1.00	≤1.50	≤0.02	≤0.04	≤1.00
Binder D22	22	3	5	<0.03					

binder powder. These reactive mixtures were then compressed into square inserts with varying thicknesses. The reactive inserts were placed into the bottom of sand moulds with a cubic cavity of 100 × 100 × 100 mm, where the SHS-reaction was ignited by the heat of the cast steel. The samples were cast in three batches, with casting temperature of 1650 °C. After casting the ingot cooled over night to room temperature inside the casting mould. Table 2 presents the compositions of the reactive inserts and displays the hard phase forming elements, the binder type and the mass percentage of the binder in the insert.

The samples were cut to study the cross-sections of the coatings. The polished cross-sections of the samples were studied using Zeiss ULTRAplus ultra high resolution field emission scanning electron microscope (UHR FEG-SEM) equipped with Oxford INCA x-act analytical silicon drift detector (SDD) and INCA Energy 350 energy dispersive analyser (EDS). All the SEM images shown in this article are backscattered electron images. Size distributions and areal fractions of TiC particles were determined by image analysis of the backscattered electron images and the average (avg.) and standard deviations (std.) were calculated for each sample. The particle size distribution and hardness values in results and discussion are given in the form "(avg. – std.) – (avg. + std.)". Vickers hardness was tested with Duramin A-300 hardness tester with 3 kg load.

3. RESULTS AND DISCUSSION

SEM-images of the coating cross-sections and hardness values of the coatings were compared, to study how the reactive insert design affects the coating micro-structure. SEM images of the coating cross-sections displayed heterogeneous microstructures, where TiC particles were finely dispersed and bonded well to the steel matrix. Molybdenum coated the TiC particles and reduced effectively the size of the TiC particles. Hardness values of the coatings were more than twice higher than those of the as-cast duplex A890 4A steel substrate. Hardness value of the steel substrate varied from 220 to 250 HV3 for all samples.

3.1. Effect of the binder type

Changing the binder type from iron to duplex stainless steel affected the TiC particle size distribution and the hardness values of the coating. TiC particle size

Table 2. Compositions of reactive inserts

Sample	Hard phase formers	Binder type	Amount of binder, wt%
1	Ti, C, Mo	Fe	25
2	Ti, C	D22	25
3	Ti, C, Mo	D22	25
4	Ti, C, Mo	D22	12
5	Ti, C, Mo	D22	8

distribution with pure iron binder (Fig. 1a) was wider (0.3–1.8 µm) with more fine particles than with D22 binder (Fig. 1b), in which the particle size distribution (1.1–1.8 µm) was narrower. The hardness values of the coating in sample 1 were 560–860 HV3, and 410–790 HV3 in sample 3. Higher average volume fraction of TiC particles in the coating of the sample 1 causes slightly higher hardness of the sample 1. Furthermore, the variation in hardness values relates to the general variation of the TiC volume fraction in the coating structure.

Figure 2 shows backscattered electron image and EDS maps of reinforcement particles taken from the same area. The EDS maps (Fig. 2b) show titanium carbide particles with molybdenum in the outer shell, chromium rich phases and steel matrix. Since the binder of sample 1 contains no chromium, the chromium in Fig. 2b originates from the cast duplex steel, which was mixed with the TiC reinforced coating during the SHS reaction.

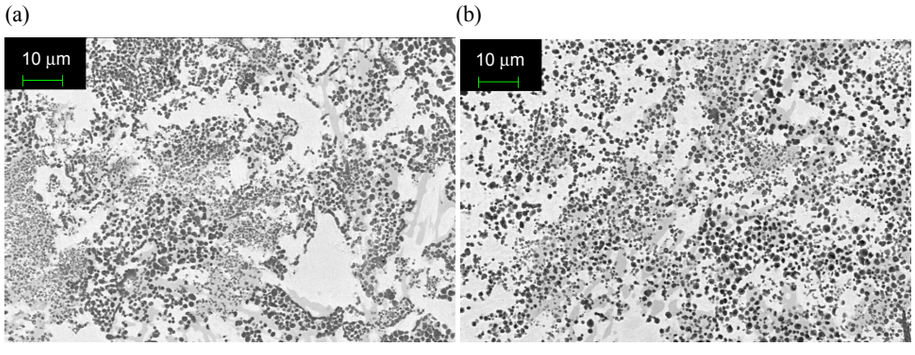

Fig. 1. SEM images of cross-sections of coatings with binder: (a) iron (sample 1); (b) duplex stainless steel (sample 3).

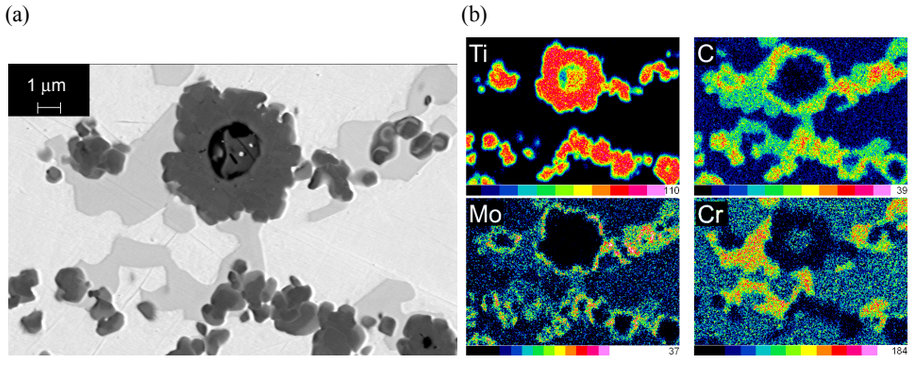

Fig. 2. (a) SEM image; (b) EDS maps of reinforcement particles in sample 1.

3.2. Effect of molybdenum

The effect of molybdenum on the formation and microstructure of titanium carbide particles was studied by adding pure molybdenum powder into the reactive insert of sample 3, but not into the reactive insert of sample 2. The addition of molybdenum in sample 3 (Fig. 3a) produced a coating with clearly smaller TiC particles than in sample 2 (Fig. 3b). The coating microstructure without molybdenum had densely packed regions of distinctly bigger sized TiC particles and pools of the matrix metal. The coating hardness values with Mo were 410–790 HV3, and without Mo 520–640 HV3. The average hardness for both is approximately the same (600 HV3).

Figure 4 shows detailed images of samples 2 and 3. TiC particles appear as dark grey. The diameter of the TiC particles, produced without molybdenum, varied from 1.8 to 2.6 µm and with molybdenum from 1.2 to 1.7 µm. EDS analysis confirmed that with the addition of molybdenum, the TiC particles were

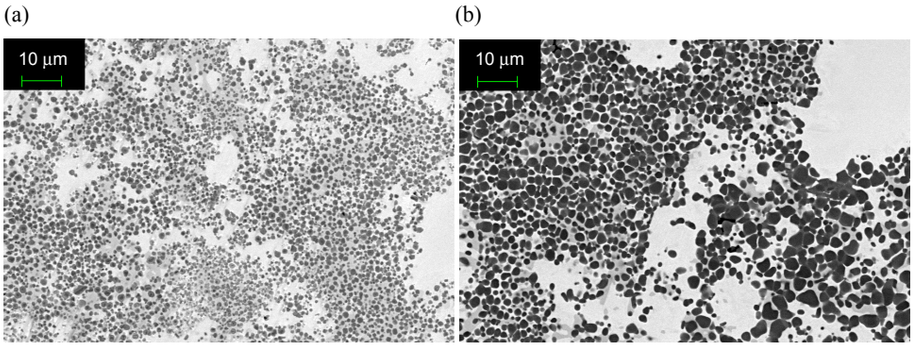

Fig. 3. SEM image of the titanium carbide particles: (a) with molybdenum (sample 3); (b) without molybdenum (sample 2).

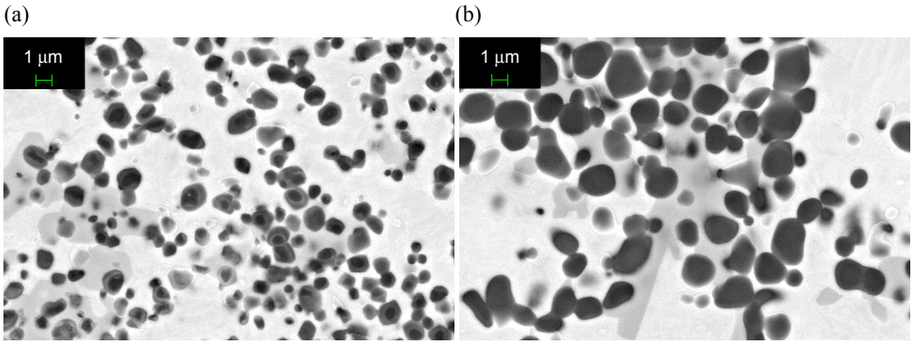

Fig. 4. SEM image of titanium carbides: (a) with molybdenum (sample 3); (b) without molybdenum (sample 2).

coated with the molybdenum enriched phase. This is in accordance with the findings in [5]. As the particle size is distinctly smaller with the addition of molybdenum, the Mo-TiC layer around the TiC nucleus restricts the growth of the TiC particles.

3.3. Effect of the amount of the binder

Reducing the amount of the binder powder in the reactive insert increases the heat, released by the SHS reaction, and this in turn reduces viscosity of the surrounding liquid steel. The reduced viscosity helps the steel to flow better between the particles, thereby increasing the interparticle distance, and reducing the average volume fraction of TiC particles in the coating. Figures 3a, 5a and 5b show how interparticle distance grows as the binder D22 amount in the reactive insert is decreased.

The hardness of the coatings varied. The values were 413–785 HV3 with 25 wt% of binder D22 (sample 3), 403–592 HV3 with 12 wt% of binder D22 (sample 4) and 350–643 HV3 with 8 wt% of binder D22 (sample 5). The higher average hardness of the sample 3 indicates, that the average volume fraction of TiC particles is distinctly higher in the coating of sample 3 than in the coatings of samples 4 and 5. This was confirmed also by image analysis.

4. CONCLUSIONS

The microstructure of the produced coatings depended on the composition of the reactive insert. By changing the composition, the reactivity, the heat and the chemistry of the exothermic reaction changed. In all analysed samples, fine TiC particles were distributed heterogeneously throughout the coating. The heterogeneous structure of the coatings caused variations to the measured hardness values. This variation was noticed to relate to the volume fraction of the hard

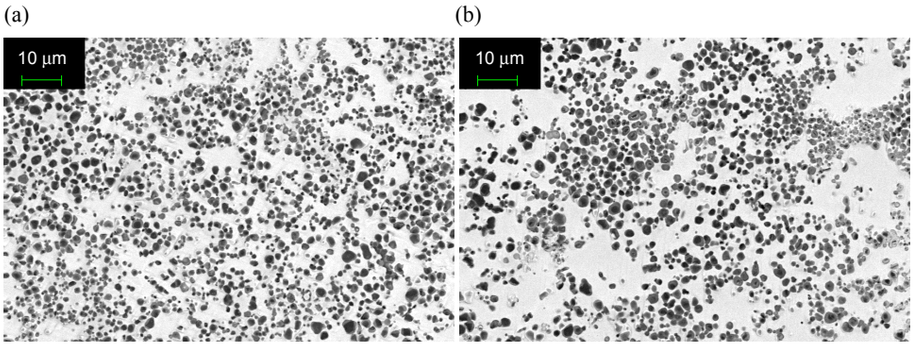

Fig. 5. SEM image of the titanium carbide particles with the amount of binder D22 equal to 12 wt%, sample 4 (a) and 8 wt%, sample 5 (b).

phase in the steel matrix. TiC particles bonded well with the metal matrix, a mixture of cast duplex steel (A890 4A) and metallic binder powder (iron or duplex stainless steel). The use of the iron binder resulted in a slightly harder coating with a wide TiC particle size distribution. Molybdenum in the reactive insert reduced clearly the particle size of TiC particles. However, reducing the binder content reduced also the hardness and areal fraction of TiC particles in the produced coating.

REFERENCES

1. Moore, J. J. and Feng, H. J. Combustion synthesis of advanced materials. Part I: Reaction parameters. *Progr. Mater. Sci.*, 1995, **39**, 243–273.
2. Moore, J. J. and Feng, H. J. Combustion synthesis of advanced materials. Part II: Classification, applications and modelling. *Progr. Mater. Sci.*, 1995, **39**, 275–316.
3. Parashivamurthy, K. I., Kumar, R. K., Seetharamu, S. and Chandrasekharaiah, M. N. Review on TiC reinforced steel composites. *J. Mater. Sci.*, 2001, **36**, 4519–4530.
4. Zhang, Z. Q., Shen, P., Wang, Y., Dong, Y. P. and Jiang, Q. C. Fabrication of TiC and TiB2 locally reinforced steel matrix composites using a Fe-Ti-B4C-C system by an SHS-casting route. *J. Mater. Sci.*, 2007, **42**, 8350–8356.
5. Choi, Y., Baik, N. I., Lee, J. S., Hong, S. I. and Hahn, Y. D. Corrosion and wear properties of TiC/Ni-Mo composites produced by direct consolidation during a self-propagating high-temperature reaction. *Compos. Sci. Technol.*, 2001, **61**, 981–986.
6. Gowtam, D. S., Ziyauddin, M., Mohape, M., Sontakke, S. S., Deshmukh, V. P. and Shah, A. K. In situ TiC-reinforced austenitic steel composite by self-propagating high temperature synthesis. *Int. J. Self-Propag. High-Temp. Synth.*, 2007, **16**, 70–78.
7. Gowtam, D. S., Rao, A. G., Mohape, M., Kathkar, V., Deshmukh, V. P. and Shah, A. K. Synthesis and characterization of in-situ reinforced Fe-TiC steel FGMs. *Int. J. Self-Propag. High-Temp. Synth.*, 2008, **17**, 227–232.
8. Kim, H. S. On the rule of mixtures for the hardness of particle reinforced composites. *Mater. Sci. Eng. A*, 2000, **A289**, 30–33.
9. Humenik, M. and Parikh, N. M. Fundamental concepts related to microstructure and physical properties of cermet systems. *J. Am. Ceram. Soc.*, 1956, **39**, 60–63.
10. Moscowitz, D. and Humenik, M. In *Modern Developments in Powder Metallurgy*. Plenum Press, New York, 1966, Vol. 3.

Funktsionaalse gradientstruktuuri formeerumine roostekindlast dupleksterasest valanditel

Jyri Tiusanen, Kati Rissa, Tapio Ritvonen, Juha Lagerbom,
Kaisu Keskiaho ja Toivo Lepistö

On uuritud titaankarbiidiosakestega tugevdatud metallmaatrikskomposiitidest pinnete formeerumist roostekindlast (austeniit/ferriit) dupleksterasest valanditel. Kulumiskindel, funktsionaalse gradientstruktuuriga metallmaatrikspinnete karbiidne (TiC) faas moodustus iseleviva kõrgtemperatuursünteesi toimel. Süntees käivitus valuterase kõrge temperatuuri (1650 °C) toimel. Paksude gradientpinnete

saamiseks valanditel vormiti valuvormi viimiseks sisetükid titaani, süsiniku, molübdeeni ja komposiitpindes sideainetena kasutatavate raua- või roostekindlast dupleksterasest pulbrite baasil. Saadud gradientstruktuuriga pinnete mikrostruktuur sõltub lähtematerjalide koostisest. Näiteks molübdeen vähendab märkimisväärselt titaankarbiidiosakeste suurust pindes. Rauast või dupleksterasest sideaine koguse vähendamine valuvormi sisetükis põhjustab tugevdava titaankarbiidi mahulise osakaalu vähenemist saadavas gradientpindes.